NUMERICAL INVESTIGATION ON DIFFERENT APPROACHES OF TWO-PARAMETER FRACTURE MECHANICS

M K Sahu[1], J, Chattopadhyay[1], B K Dutta[1], K K Vaze[1]
[1]Reactor Safety Division, Bhabha Atomic Research Centre, Mumbai, INDIA-400085
E-mail of corresponding author: mksahu@barc.gov.in

ABSTRACT

It is well established that the initiation toughness J_{IC} is relatively insensitive to geometry and loading conditions but the slope of the J-R curve (tearing modulus) is highly dependent. When the region ahead of crack tip enters in the regime of Large Scale Yielding (LSY), crack tip condition cannot be characterized by single parameter fracture mechanics. These evolve in the introduction of a second parameter to characterize the crack tip conditions. The second parameter quantifies the stress triaxiality level ahead of crack tip in remaining ligament. High level of stress triaxiality defines the uniform hydrostatic shift of the stress field ahead of crack tip which is responsible for hindering the plastic deformation. In this paper, different stress triaxiality parameters, Q and h have been investigated using Finite Element Analysis (FEA) for Centre Cracked Plate (CCP) fracture specimen. Modified Boundary Layer (MBL) analysis is validated for different power law material properties and also studied for SA333Gr6 material fitted on Ramberg-Osgood relation. Q and h are studied extensively under one of the lower constrained fracture specimen, CCP. The variation of Q and h are studied extensively with varying crack size and loading. The variation of *Q* and h are presented ahead of crack tip, along the remaining ligament and a unique linear relationship is established.

INTRODUCTION

One of the most widely used constraint indexing parameter is the stress triaxiality factor (*h*)[1], which is defined by the ratio of hydrostatic or mean stress (σ_m), which does not cause any plastic deformation, to the von-Mises equivalent stress (σ_e), which is being responsible for plastic deformation. Stress triaxiality factor is defined as,

$$h = \sigma_m / \sigma_e \tag{1}$$

Where,

$$\sigma_m = (\sigma_1 + \sigma_2 + \sigma_3)/3 \tag{2}$$

$$\sigma_e = \left[(\sigma_1 - \sigma_2)^2 + (\sigma_2 - \sigma_3)^2 + (\sigma_3 - \sigma_1)^2 \right]^{1/2} \Big/ \sqrt{2} \tag{3}$$

σ_1, σ_2 and σ_3 are the principal stresses.
O'Dowd and Shih [2] and most subsequent researchers defined Q as follows,

$$Q = \frac{\sigma_{\theta\theta} - (\sigma_{\theta\theta})_{SSY,T=0}}{\sigma_0} \quad \text{at } \theta = 0^\circ \text{ and } r/(J/\sigma_0) = 2 \tag{4}$$

Where σ_0 is the yield stress and $\sigma_{\theta\theta}$ is the hoop stress around the crack tip. $[(\sigma_{\theta\theta})_{SSY,T=0}]$ is the reference stress computed using Small Scale Yielding (SSY) and keeping Transverse stress(T) equal to zero.

Q solutions can be derived either using HRR field or SSY field as reference field distribution. It was found that when SSY solution is chosen as the reference field, the difference fields correspond more closely to a uniform hydrostatic stress state over a greater range of plastic deformation. However the choice of reference field used in the definition in above equation of Q is a matter of convenience. O'Dowd and Shih emphasized that once the choice is made, it must be carried out consistently throughout the analysis. They recommended that above equation be used as the standard definition for Q with the small strain solution as the reference field. Having a standard definition facilitates the comparison of solutions obtained by different investigators and tabulation of handbook of 'Q' solutions. In the present work, SSY is chosen as the reference field.

THE MODIFIED BOUNDRY LAYER (MBL) ANALYSIS

The reference field in Eq. 4 is computed by means of a standard boundary layer solution. A half circular finite element mesh having outer boundary radius 'R' (in this analysis R=1000mm) is used for this purpose. On the boundary of this model, displacements corresponding to elastic solution are applied as per Eq. 5 and 6. A plastic zone develops at the crack tip, but its size must be small (between 0.01R to 0.1R) relative to the size of the model.

This configuration is referred to as Modified Boundary Layer (MBL) analysis, which simulates the near tip conditions in an arbitrary geometry, provided the plasticity is well contained within the body. It is equivalent to removing a core region from the crack tip and constructing a free body diagram as shown in Figure 1[3].

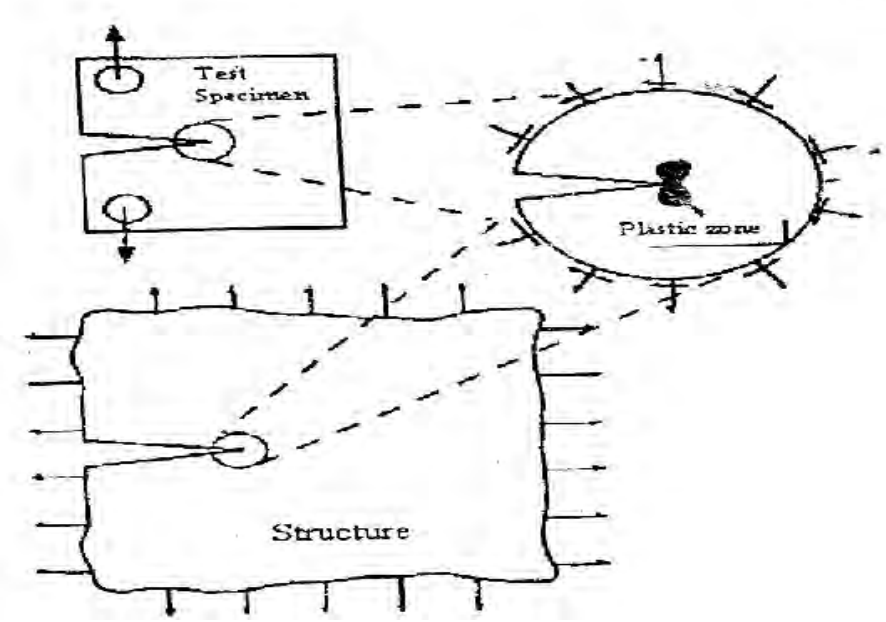

Figure 1. Test specimen and structure loaded to same stress intensity.

Two dimensional plane strain finite element analysis are conducted to obtain very detailed resolution of the crack tip stress fields for the MBL model.

Mesh and Boundary Conditions

The reference field in Eq.4 has been computed in the vicinity of crack tip, where the stress gradient is high. Hence, very fine mesh is required to capture the stress field accurately. Meshing consists of 1200 elements and 3741 nodes. Eight noded isoparametric quadrilateral elements are used. Reduced integration is employed in all elements. This model has 30 elements in the circumferential and 40 elements in the radial direction, respectively. Symmetry boundary conditions are applied on the plane y = 0. These models are loaded by imposing displacement increments of the elastic singular field for mode I on the outer circular boundary as per Eq.5 and 6.

$$\Delta u(r,\theta) = \frac{1+\nu}{E}\,\Delta KI\left(\frac{r}{2\pi}\right)0.5\,(3-4\nu-\cos\theta)\cos(\theta/2) \quad (5)$$

$$\Delta v(r,\theta) = \frac{1+\nu}{E}\,\Delta KI\left(\frac{r}{2\pi}\right)0.5\,(3-4\nu-\cos\theta)\sin(\theta/2) \quad (6)$$

Material Parameters

The uniaxial stress strain curve follows Ramberg Osgood form.

$$\left(\frac{\varepsilon}{\varepsilon_0}\right) = \left(\frac{\sigma}{\sigma_0}\right) + \alpha\left(\frac{\sigma}{\sigma_0}\right)^n$$

Where,

ε is true strain,
σ is the true stress,
σ_0 is the yield stress (0.2 % offset value)
$\varepsilon_0 = \sigma_0 / E$, E is Young's modulus,
α is the Ramberg-Osgood coefficient,
n is the strain hardening exponent.

Different strain hardening exponents, n = 3,5,10 and 20 are chosen which cover the range of structural steels from high strain hardening to ideal plastic materials. n = 3 to 5 covers the range for carbon steels, n = 5 to 10 for stainless steels and n = 20 for ideal plastic materials. The Ramberg-Osgood coefficient 'α' is assigned a value of '1' for a piecewise power law material. The other properties typical of those for moderate strength structural steels are adopted in computation. ($\varepsilon 0 = 1/500$, $\sigma 0 = 400$ Mpa and $\nu = 0.3$)
The analysis has also been carried out for Indian PHWR PHT material (SA 333 Gr6). The material properties at the temperature of 250˚ C are given in Table 1.

Table 1. Material Properties for Indian PHWR material (SA 333 Gr6)

Material Properties	Value
Yield stress, σo	240 MPa
Young's modulus of elasticity, E	188 GPa
Poisson's ratio, υ	0.3
Strain hardening exponent, n	3.273
Ramberg Osgood coefficient, α	8.1505

Results of MBL Analysis

The plastic zone size increases as K_I increases. But this has to be limited to ensure Small Scale Yielding (SSY) conditions. As per this criteria, the plastic zone size is not allowed to increase beyond 0.1 R[4]. Reference stress $[(\sigma_{\theta\theta})_{ref}]$ has been calculated at a distance of $cJ/\sigma 0$ (c = 1,2,3,4,5) ahead of crack tip at different angular positions in the forward sector ($\theta \leq 90^{\circ}$). The results obtained are compared with the available literature. Table 2 and Table 3 summarize the reference stresses for piece wise power law material and Indian PHWR material respectively.

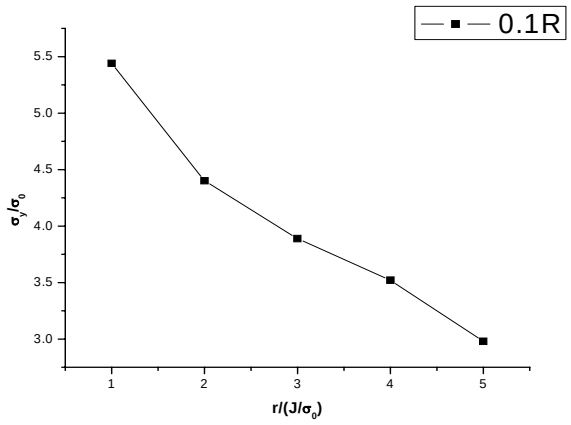

Figure 2. Reference Stresses evaluated using MBL at θ=0.

FINITE ELEMENT ANALYSIS OF CCP FOR STRESS TRIAXIIALITY PARAMETER, 'Q'

Finite Element Model

Figure 3 (a), Shows schematic drawing of CCP geometry used in the current study. Due to symmetry in both geometry and loading conditions, only $1/4^{th}$ of the CCP is modeled (See Figure 3 (b)). Different finite element models are constructed for each of a/w ratios investigated. Eight noded plain strain isoparametric quadrilateral elements are used. Reduced (2x2) Gaussian integration is used to eliminate locking of arbitrarily shaped elements. Since the crack tip region contains steep stress and strain gradients, the mesh refinement should be more at the crack tip. The spider web meshing facilitates a smooth transition from a fine mesh at the crack tip to a coarse mesh remote to the crack tip. In the present work, all the models used spider web meshing near the crack-tip. This spider meshing consists of 20 elements in circumferential direction and 30 elements in radial direction. Figure 3 (c) shows the typical finite element meshes used for this analysis. It also depicts a close up at the crack tip region. Symmetry

boundary conditions are applied on the CCP at y = 0.0 and x = 0.0 (except at the cracked line). A uniform tensile loading is imposed on the CCP geometry.

Table 2. Reference stresses, $(\sigma_{\theta\theta})_{ref}/\sigma_0$ obtained from SSY, T=0 solution for a piecewise power law material. (a) n = 3, (b) n = 5, (c) n = 10, (d) n = 20 respectively.

(a)

$r/(J/\sigma_0)$	θ=0˚ (OS*)	θ=0˚	θ=24˚	θ=30˚	θ=42˚	θ=60˚	θ=66˚	θ=84˚	θ=90˚
1	5.46	5.44	5.12	4.95	4.53	3.74	3.46	2.57	2.27
2	4.53	4.40	4.19	4.06	3.72	3.08	2.84	2.09	1.83
3	4.06	3.89	3.74	3.64	3.34	2.76	2.55	1.90	1.68
4	3.76	3.52	3.48	3.44	3.21	2.65	2.44	1.73	1.50
5	3.53	2.98	2.54	2.50	2.66	2.17	2.02	1.61	1.47

(b)

$r/(J/\sigma_0)$	θ=0˚ (OS*)	θ=0˚	θ=24˚	θ=30˚	θ=42˚	θ=60˚	θ=66˚	θ=84˚	θ=90˚
1	4.42	4.44	4.21	4.04	3.70	3.09	2.87	2.19	1.96
2	3.90	3.87	3.70	3.57	3.28	2.74	2.55	1.96	1.74
3	3.63	3.58	3.45	3.34	3.07	2.58	2.39	1.84	1.65
4	3.44	3.37	3.28	3.20	2.96	2.47	2.29	1.75	1.56
5	3.29	2.81	2.60	2.58	2.60	2.08	1.96	1.64	1.48

(c)

$r/(J/\sigma_0)$	θ=0˚ (OS*)	θ=0˚	θ=24˚	θ=30˚	θ=42˚	θ=60˚	θ=66˚	θ=84˚	θ=90˚
1	3.57	3.65	3.43	3.31	3.02	2.55	2.39	1.88	1.71
2	3.35	3.38	3.20	3.10	2.85	2.41	2.26	1.77	1.61
3	3.22	3.23	3.07	2.98	2.74	2.31	2.16	1.71	1.55
4	3.12	3.13	2.99	2.91	2.68	2.26	2.11	1.66	1.51
5	3.03	2.71	2.54	2.53	2.41	1.89	1.79	1.55	1.40

(d)

$r/(J/\sigma_0)$	θ=0˚ (OS*)	θ=0˚	θ=24˚	θ=30˚	θ=42˚	θ=60˚	θ=66˚	θ=84˚	θ=90˚
1	3.21	3.27	3.07	2.96	2.71	2.30	2.16	1.73	1.58
2	3.09	3.12	2.95	2.85	2.62	2.22	2.08	1.67	1.52
3	3.01	3.03	2.87	2.78	2.56	2.17	2.03	1.62	1.48
4	2.95	2.94	2.82	2.73	2.51	2.12	1.99	1.59	1.44
5	2.89	2.58	2.36	2.28	2.27	1.78	1.68	1.41	1.24

*OS= Odowd and Shih

Table 3. Reference stresses, $(\sigma_{\theta\theta})_{ref} / \sigma_0$ obtained from SSY, T=0 solution for Indian PHWR material at $\theta=0^{\circ}$

$r/(J/\sigma_0)$	1	2	3	4	5
$(\sigma_{\theta\theta})_{ref}/\sigma_0$	3.60	3.16	3.00	2.92	2.85

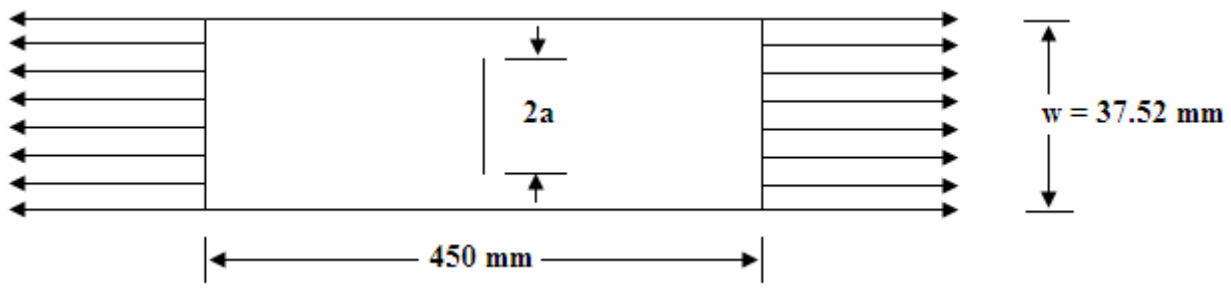

(a)

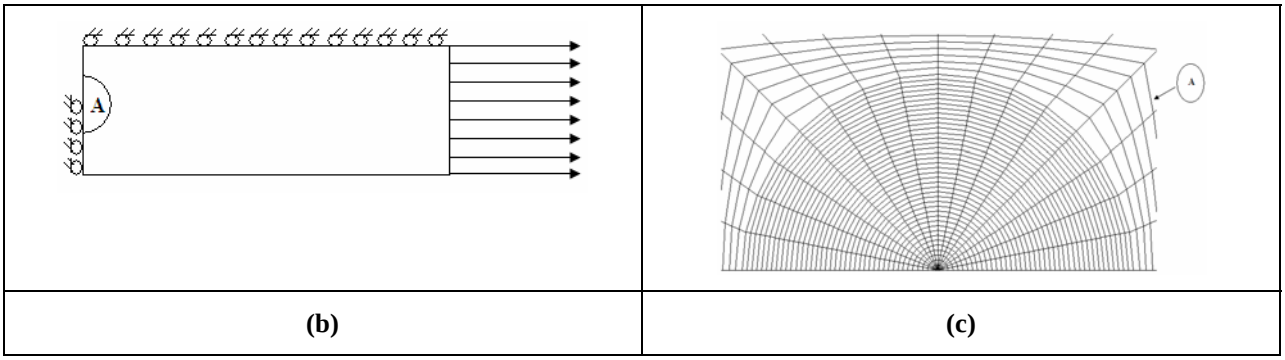

(b) **(c)**

Figure 3. Detail of standard CCP specimen. (a) Schematic diagram (b) 1/4th models is used with appropriate symmetricity . (c) Finite element mesh showing details of crack tip region.

For a piecewise power law material, *Q* is computed and compared with the other literature data. However data is showing significant deviation with Odowd and Shih at lower deformation level but they are in comparatively good agreement at higher deformation level. Present analysis is showing good agreement with Pawan Kumar et. al.[3].

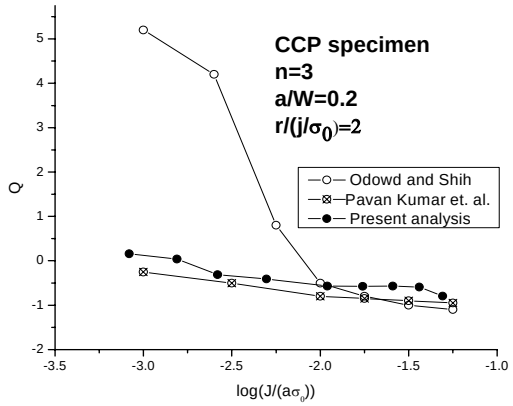

Figure 4. Comparison of Q for CCP specimen

Determination of Q for Indian PHWR material:

The 'Q' solutions are reported for Centered Cracked Panel (CCP) geometry. The 'Q' parameter and triaxiality factor (h) are evaluated at a distance of cJ/σ_o (c = 1, 2, 3, 4, 5) along crack line ($\theta = 0^\circ$).

The crack opening stress (σ_{yy}, $\theta = 0^\circ$) field ahead of the crack tip is shown in Figure 5 for Indian PHWR PHT material.The stress field is compared with the SSY solution at different deformation levels for different a/W ratios.Figure 6 shows the typical variation of 'Q' with distance over the range of J/σ_0 to 5 J/σ_0 along the crack line ($\theta = 0^\circ$) for Indian PHWR PHT material. 'Q' is almost independent of distance but dependence on applied loading is evident, irrespective of crack depth.

The variation of triaxiality factor 'h' with distance (J/σ_0 to 5 J/σ_0) along crack line is plotted in Figure 7. The triaxiality factor values are compared with that of SSY solution at different deformation levels. The values fall below that of SSY solution, irrespective of crack depth. Centered Cracked Panel (CCP) geometry maintains low stress triaxiality when compared with SSY solution. Hence CCP can be treated as low constraint geometry. Unlike the 'Q' parameter, 'h' parameter shows strong dependence on distance ahead of crack tip. The variation of Q with respect to h is tried to plot for CCP specimen. The values are taken at a characteristic distance of $2J/\sigma_0$ for different loading conditions and for different a/w ratios. A unique linear fit is shown in Figure 8.

CONCLUSION

For a piecewise power law material, Using modified boundary layer analysis the reference stress (for SSY and T=0) is computed and compared with literature data and found in good agreement. Reference stress and stress triaxiality factor (h) is s also computed for Indian PHWR material. For a CCP specimen, stress triaxiality parameter (Q) is computed using piecewise power law material. The result is compared with literature data and found in reasonably good agreement. Using Indian PHWR material, Q and h are computed for different a/w ratios (0.05, 0.15, 0.25 and 0.35). For specific a/w ratio, the variation of Q and h are plotted with loading. It is found that on increasing loading the stress triaxiality parameters are decreasing initially with rapid rate. On further increasing load, the value of stress triaxiality is being asymptotic. A unique linear relationship is proposed between Q and h for CCP specimen.

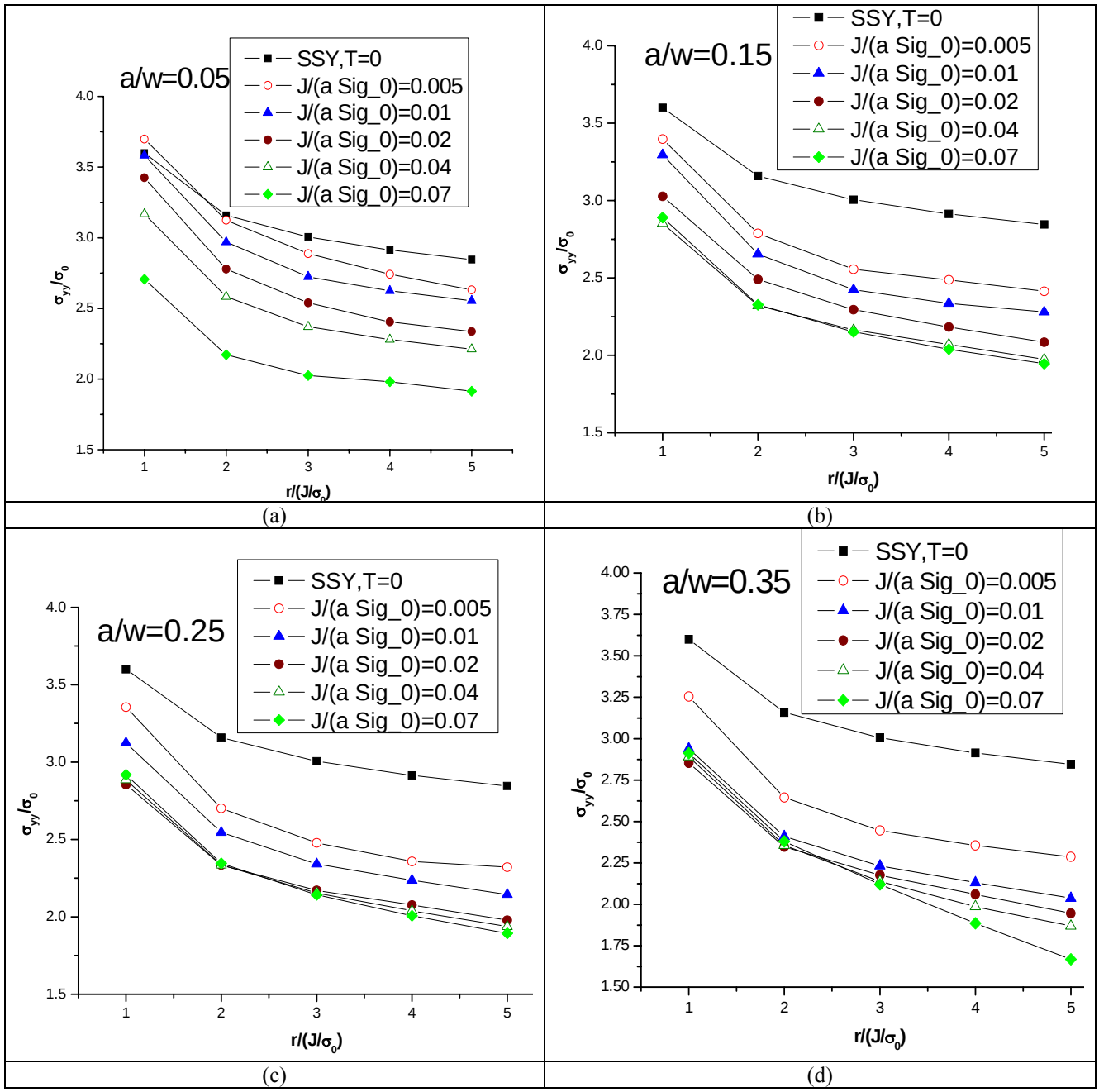

Figure 5. Variation of crack opening stress with distance ahead of crack tip (a) a/w=0.05, (b) a/w=0.15, (c) a/w=0.25 and (d) a/w=0.35

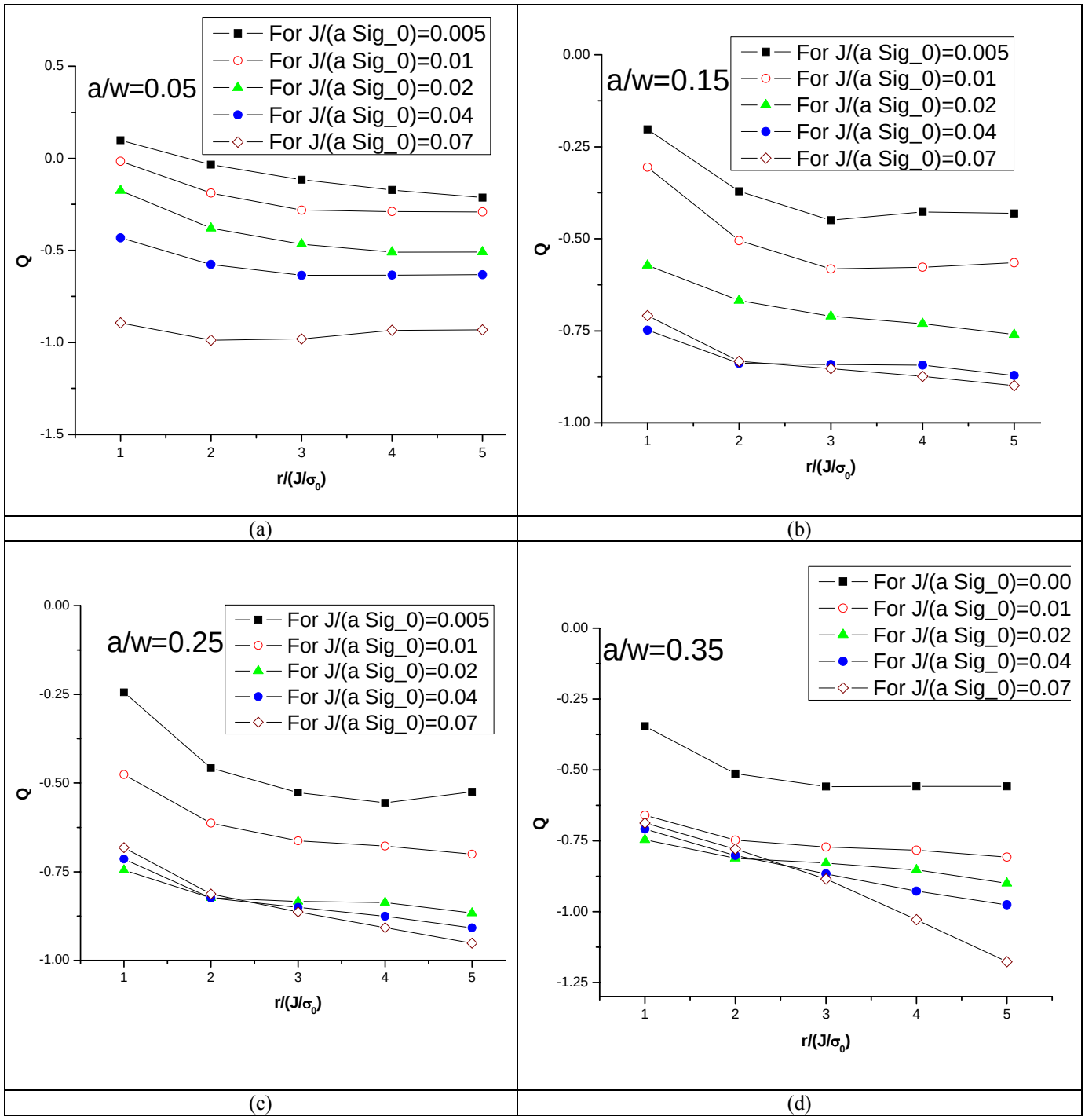

Figure 6. Variation of 'Q' with distance at different deformation levels. (a) a/w=0.05, (b) a/w=0.15, (c) a/w=0.25 and (d) a/w=0.35

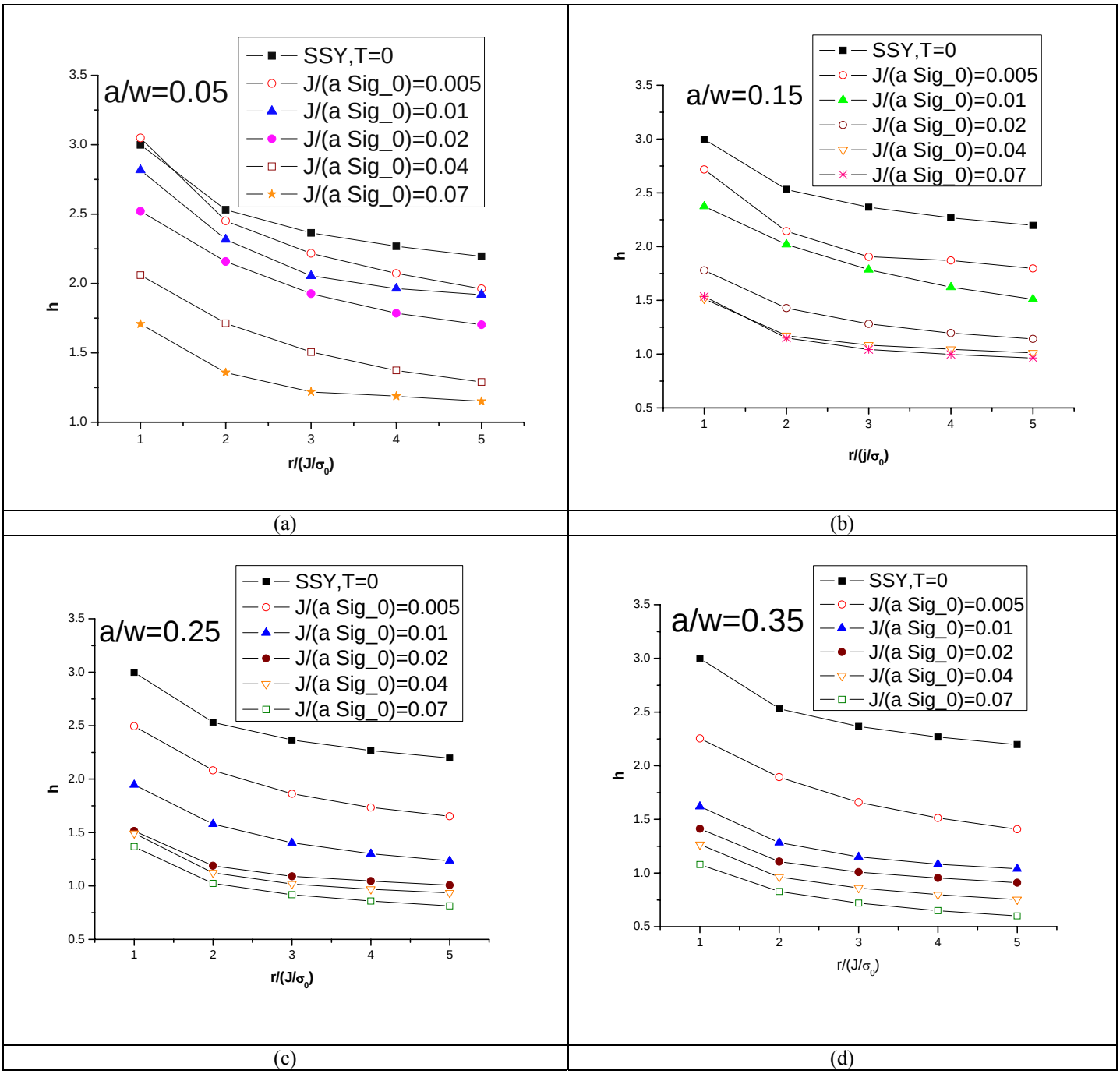

Figure 7. Variation of 'h' with distance at different deformation levels. (a) a/w=0.05, (b) a/w=0.15, (c) a/w=0.25 and (d) a/w=0.35

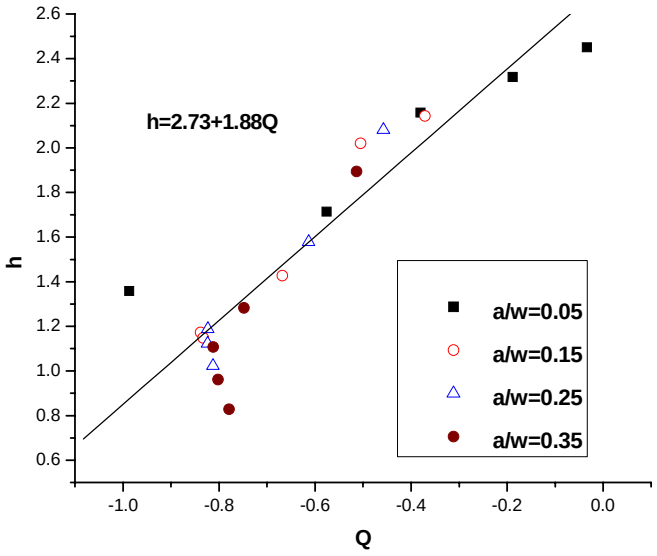

Figure 8. Variation of h with Q for low constraint geometry

REFERENCES

[1]. W. Brocks, G. Kunecke, H. D. Noack, & H. Veith, "On the transferability of fracture mechanics to structures using FWM", Nuclear Engineering and Design, Vol.112, 1989, pp-1-14.

[2]. O'Dowd NP, Shih CF, "Family of crack tip fields characterized by a triaxiality parameter–I: structure of fields", J Mech Phys Solids. Vol. 39,1991, pp. 898-101

[3]. T. V. Pawankumar, J. Chattopadhyay, B. K. Dutta, " Study of crack tip constraint parameters in two dimensional geometries", Bhabha Atomic Research Centre, Technical report, 1998

[4]. R. H. Dodds, T.L. Andsrson, and M. T. Kirk, " A framework for correlate a/w effects on elastic plastic fracture toughness (J_c)", International Journal of Fracture, Vol.48, 1991, pp. 1-22.